Incorporation of zirconia particles into coatings formed on magnesium by plasma electrolytic oxidation

R. Arrabal · E. Matykina · P. Skeldon ·
G. E. Thompson

Abstract The incorporation of particles of monoclinic zirconia into coatings formed on magnesium by plasma electrolytic oxidation has been examined in order to investigate the mechanism of coating formation. The coatings, developed under DC conditions in alkaline silicate and phosphate electrolytes, comprised two main layers and contained MgO, Mg_2SiO_4, and $Mg_3(PO_4)_2$ phases. Zirconia particles were incorporated preferentially into the inner layer regions and at the coating surface. Zirconium was also redistributed in the outer layer coating material, sometimes resulting in a modified microstructure. Due to local heating at the microdischarge sites, particles underwent transformation from monoclinic to tetragonal zirconia, although monoclinic zirconia was also present in the final coating. $Mg_2Zr_5O_{12}$ was also formed in the coating produced in phosphate electrolyte. The findings suggest that the outer coating material forms at the inner/outer coating interface region and the coating surface, with transport of particles to the former region through short-circuit paths in the outer layer.

Introduction

Plasma electrolytic oxidation (PEO) is being developed and applied for surface finishing of light metals. The process produces relatively thick, ceramic-like coatings containing amorphous and crystalline phases, with incorporation of species originating from the substrate and the electrolyte [1–4]. The coating growth takes place above the dielectric breakdown voltage of the coating, when short-lived microdischarges occur locally on the coating surface. The coatings may be formed under DC or AC conditions [5, 6]. The coating formation is usually considered to involve anodic oxidation, thermal oxidation, and plasma chemical mechanisms that occur at high local temperatures [7].

As a contribution to the understanding of the mechanisms of coating formation, the authors have recently employed a tracer approach involving sequential DC PEO treatments in two electrolytes of different compositions. Coatings with layered compositions have been shown to result on aluminum sequentially treated in phosphate and silicate electrolytes, with transport of anion species of the second electrolyte to the inner coating regions along short-circuit paths [8, 9]. Work of the authors on magnesium alloy WE43-T6 has revealed a similar behavior, with anionic constituents of the electrolyte reaching the inner coating regions by short-circuit transport through the outer layer [10]. Studies of coatings formed in electrolytes with suspended particles offer another route to understanding the mechanisms of coating formation. Such studies are relatively few, compared with the research on coatings grown in particle-free electrolytes. Further, their focus is on improved thermomechanical properties, reduced porosity and enhanced wear resistance of the coatings, rather than mechanistic aspects [11–14]. The main work reported in the scientific literature has been carried out on aluminum. However, PEO of AM60B magnesium alloy, using alkaline phosphate electrolyte with addition of titania sol [15], has been shown to incorporate anatase and rutile into coatings. The incorporation process was suggested to involve decomposition, condensation, dehydration, and crystallization of the sol.

R. Arrabal · E. Matykina · P. Skeldon (✉) · G. E. Thompson
Corrosion and Protection Centre, School of Materials,
The University of Manchester, Sackville Street, P.O. Box 88,
Manchester M60 1QD, UK
e-mail: peter.skeldon@manchester.ac.uk

In the present study, coating growth on magnesium is explored using an electrolyte containing sub-micron particles of zirconia, with individual and sequential PEO treatments in silicate and phosphate electrolytes. Zirconia is polymorphic, occurring in monoclinic, tetragonal, and cubic structures, and hence may be an indicator of temperatures associated with microdischarges. Zirconia-containing coatings may also be of interest as a composite ceramic material, since magnesium and zirconium oxides are widely used in a variety of refractory and thermomechanical applications [16–19].

Experimental

PEO treatments

Specimens of magnesium of 99.9% purity (70 ppm Al, 20 ppm Cu, 280 ppm Fe, 170 ppm Mn, <10 ppm Ni, 50 ppm Si, <20 ppm Zn) were embedded in resin, with electrical connection provided through a copper wire. The exposed surface, of area 1 cm^2, was ground to 1,200 grit SiC, using water as a lubricant, degreased in ethanol, rinsed in deionized water, and dried in warm air. Either 0.025 M $Na_2SiO_3 \cdot 5H_2O$/0.05 M KOH, with pH 12 and conductivity 15.90 mS cm^{-1}, or 0.025 M $Na_3PO_4 \cdot 12H_2O$/1.5 M NH_4OH, with pH 12 and conductivity 7.21 mS cm^{-1}, were employed as electrolytes for formation of the coatings. The electrolytes were prepared from deionized water and high-purity chemicals. Additions of 2 g/L of monoclinic zirconia particles, of size 150–300 nm, were made as required. PEO treatments were carried out at 3 A dm^{-2}, which is in the typical range of current densities used for DC treatments, for selected times up to 2,400 s, with electrolyte stirring, using a 1 L double-walled glass cell through which a cooled water/glycol mixture was pumped in order to maintain the electrolyte temperature close to 293 K. A sheet of type 304 stainless steel, of dimensions 7.5 × 15 cm, was used as a cathode. Voltage and current signals were recorded electronically, with a sampling time of 20 ms, employing an SCXI data acquisition system (National Instruments) with data analysis by Igor Pro (Wavemetrics). After coating, specimens were rinsed with deionized water and dried in warm air.

Specimen examination

Plasma electrolytic oxidation (PEO)-treated specimens were examined by scanning electron microscopy (SEM) and field emission gun SEM (FEG-SEM), using Amray 1810 and Philips XL30 instruments respectively, both equipped with EDX analysis facilities. Cross-sections were ground through successive grades of SiC paper, followed by finishing to 1 µm diamond. Thickness measurements were made for each coating using an eddy current meter (Fisherscope Permascope), with the average of 10 measurements cited. Phase composition was investigated by X-ray diffraction (XRD), using a Philips X́Pert-MPD (PW 3040) instrument with a step size 0.005° and a scan range from 5° to 85° (in 2θ).

Results

The addition of the zirconia particles to the silicate and phosphate electrolytes had small influences on the voltage response during PEO treatment for 2,400 s in the individual electrolytes, which were evident as a steeper voltage rise in the initial ~200 s and slightly reduced final voltage in the presence of the particles (Fig. 1a, b). In the absence of zirconia, visible sparking was detected from ~170 V and ~225 V in the silicate and phosphate electrolyte
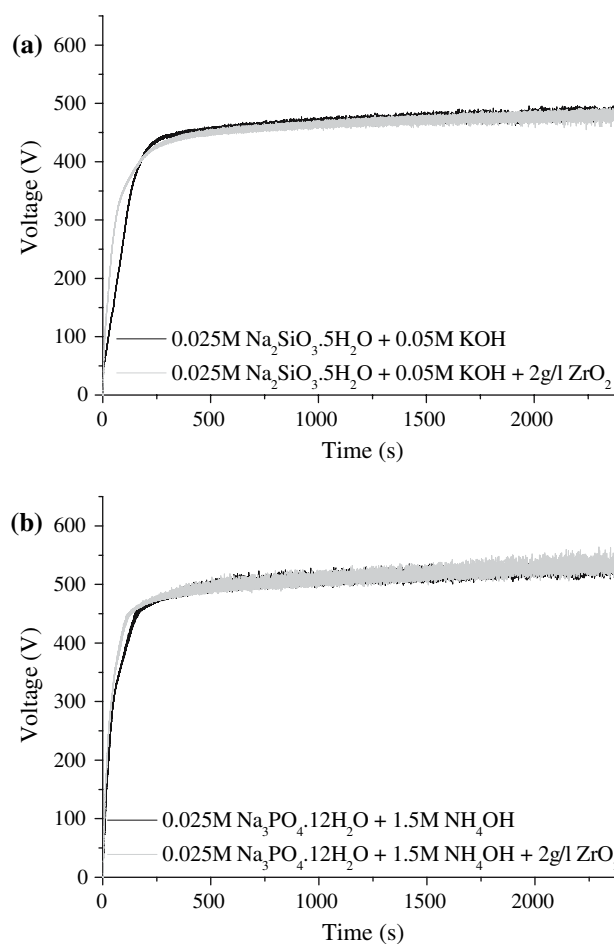
Fig. 1 Voltage time responses for PEO treatment of magnesium for 2,400 s at 3 A dm^{-2} in (**a**) 0.025 M $Na_2SiO_3 \cdot 5H_2O$/0.05 M KOH and (**b**) 0.025 M $Na_3PO_4 \cdot 12H_2O$/1.5 M NH_4OH electrolytes, with and without addition of 2 g L^{-1} of zirconia particles

respectively. Opacity of the electrolytes prevented viewing of coatings during PEO with zirconia present. The average coating thicknesses, to an accuracy of $\sim 10\%$, were ~ 15 and 37 μm following treatment in the silicate and phosphate electrolytes respectively, with negligible influence of zirconia additions to the electrolytes.

MgO, Mg_2SiO_4, and $Mg_3(PO_4)_2$ were identified by XRD in the resultant coatings, independent of the presence of particles in the electrolyte (Fig. 2a, b). Monoclinic zirconia and tetragonal zirconia were detected in coatings formed in the presence of particles, indicating transformation of the initial monoclinic zirconia during the PEO treatment; $Mg_2Zr_5O_{12}$ was additionally found for coatings formed in phosphate electrolyte.

Cross-sections revealed layered coatings for both the silicate and phosphate electrolytes in the absence of added particles (Fig. 3a–c). The outer coating material, containing relatively large voids, is permeated by channels and cracks produced by microdischarges. The inner coating
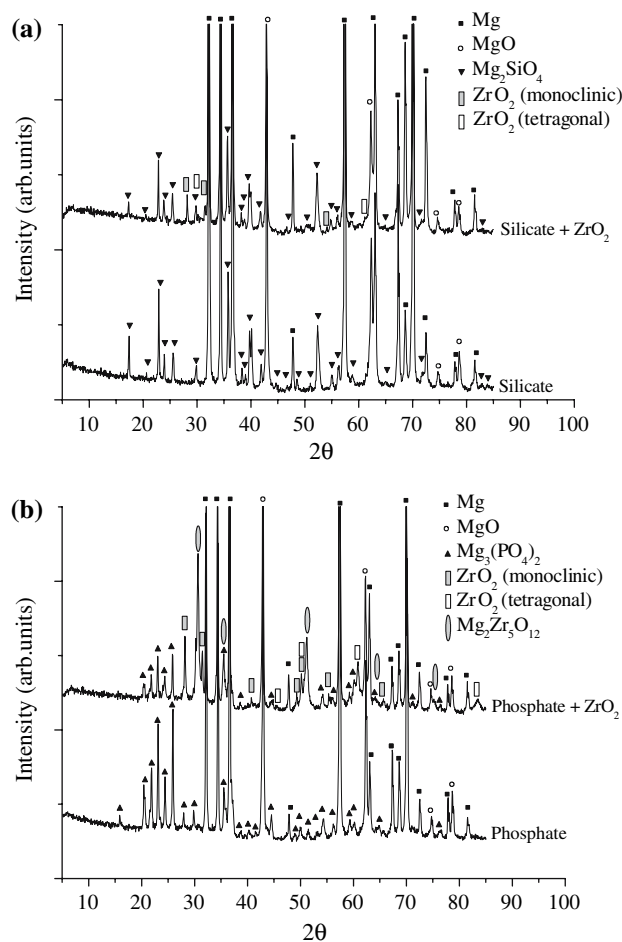

Fig. 2 XRD patterns of magnesium following PEO treatment for 2,400 s at 3 A dm^{-2} in (a) 0.025 M $Na_2SiO_3 \cdot 5H_2O$/0.05 M KOH and (b) 0.025 M $Na_3PO_4 \cdot 12H_2O$/1.5 M NH_4OH electrolytes, with and without addition of 2 g L^{-1} of zirconia particles
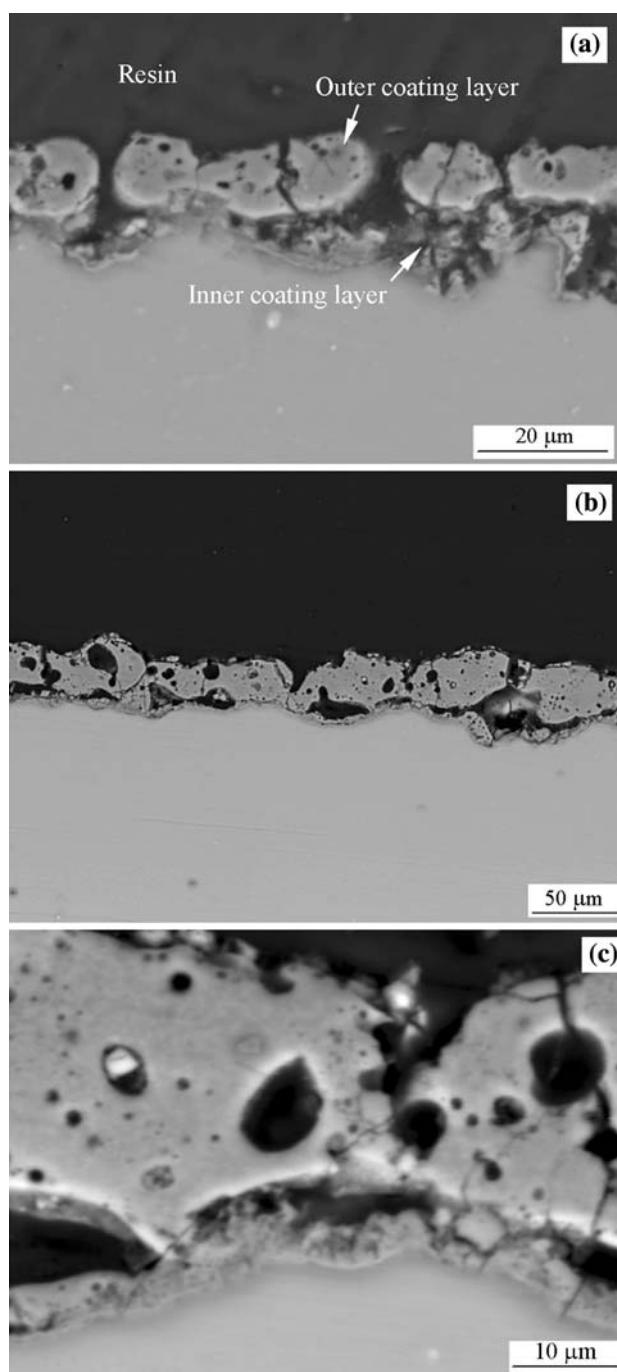

Fig. 3 Scanning electron micrographs (secondary electrons) of cross-sections of magnesium following PEO treatment for 2,400 s at 3 A dm^{-2}: (a) 0.025 M $Na_2SiO_3 \cdot 5H_2O$/0.05 M KOH; (b) 0.025 M $Na_3PO_4 \cdot 12H_2O$/1.5 M NH_4OH electrolytes; (c) detail of coating of (b)

material is more finely textured and often contained within large cavities between the substrate and the outer layer. The inner material in the coating formed in phosphate electrolyte is seen more clearly in the enlargement of Fig. 3c. Some inner layer material may be dislodged during preparation of the cross-section. According to EDX

analysis, silicon and phosphorus species are present throughout the coating thickness, although amounts of phosphorus species are less in the inner regions. A thin, relatively continuous layer is present at the metal/coating interface.

Similarly layered coatings resulted from treatments in the zirconia-containing electrolyte (Fig. 4a, b). Backscattered electron micrographs also disclosed discrete light regions due to incorporation of zirconia particles, which were especially concentrated in the inner coating material and at the coating surface. The particles appeared to be absent from the thin coating layer at the metal/coating interface. Occasional particles in the outer coating material may be due to translocation from the inner material during polishing. X-ray mapping of the coatings formed in the silicate and phosphate electrolytes indicated a general presence of zirconium in the outer layer, in addition to discrete zirconia particles (Fig. 4c, d). Signals from the inner coating regions appeared to be associated mainly with zirconia particles. Part of the X-ray signal arises

from phosphorus in the coatings, which produces X-rays of similar energy to those from zirconium. However, energy-dispersive X-ray point analyses of the outer layers indicated a much-increased total signal for the coatings incorporating zirconia particles, consistent with the significant presence of zirconium species in these regions. Further, for the coating formed in the phosphate electrolyte, scanning electron micrographs at increased magnification revealed features suggestive of a mixed phase microstructure in the outer coating produced in the zirconia-containing phosphate electrolyte (Fig. 4e). In contrast, the outer coating material produced in silicate was uniform in appearance at the resolution of the images, for both zirconia-containing and zirconia-free electrolytes.

Plan view imaging of the coating surface formed in phosphate electrolyte revealed non-uniformly distributed zirconia particles (Fig. 5). In some regions, the particles covered most of the coating surface; at other regions, the particles were less numerous, and cavities were present in the coating of similar size to the particles. The cause of the

Fig. 4 Scanning electron micrographs (backscattered electrons) of cross-sections of magnesium following PEO treatment for 2,400 s at 3 A dm^{-2} in (a) 0.025 M Na$_2$SiO$_3$ · 5H$_2$O/0.05 M KOH and (b) 0.025 M Na$_3$PO$_4$ · 12H$_2$O/1.5 M NH$_4$OH electrolytes, with addition of 2 g L^{-1} of zirconia particles. (c, d) EDX elemental maps of distributions of zirconium in coatings of (a) and (b) respectively. (e) Details of outer coating region of (b)
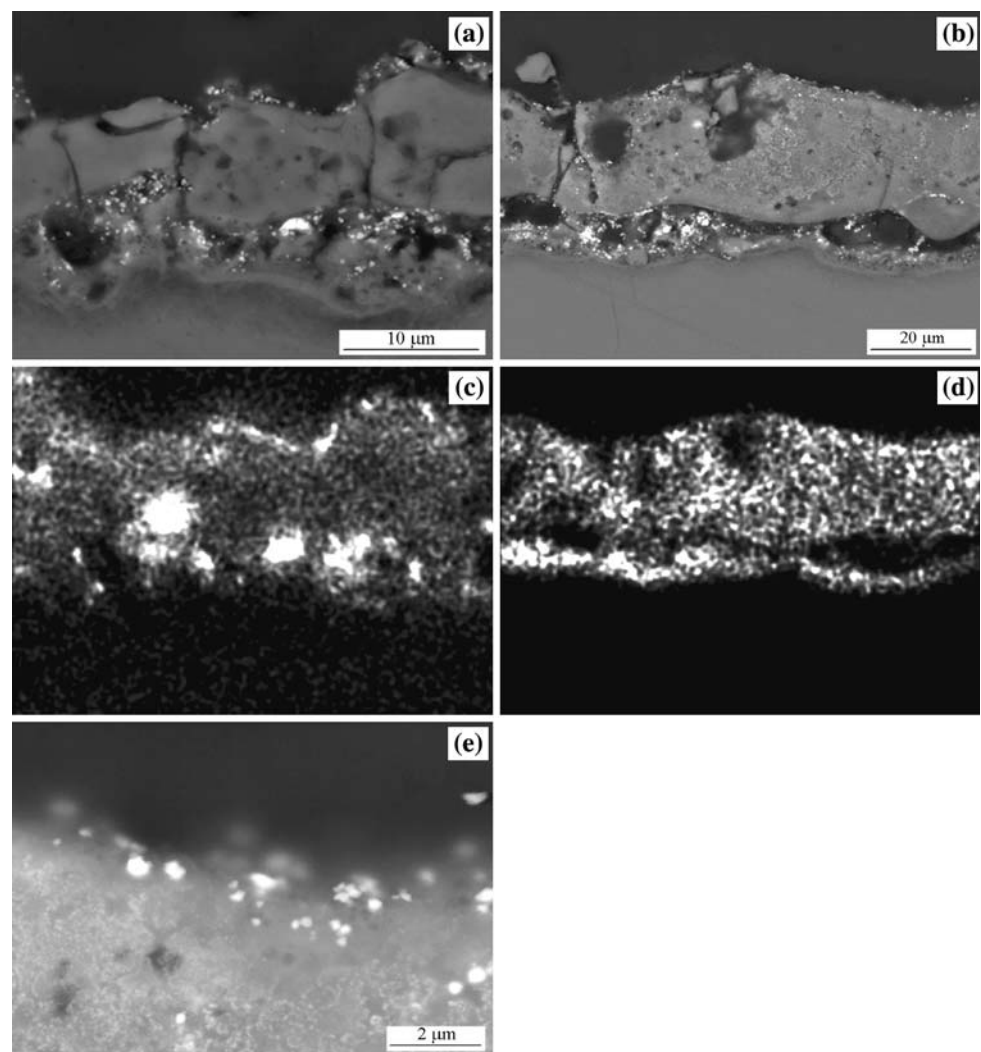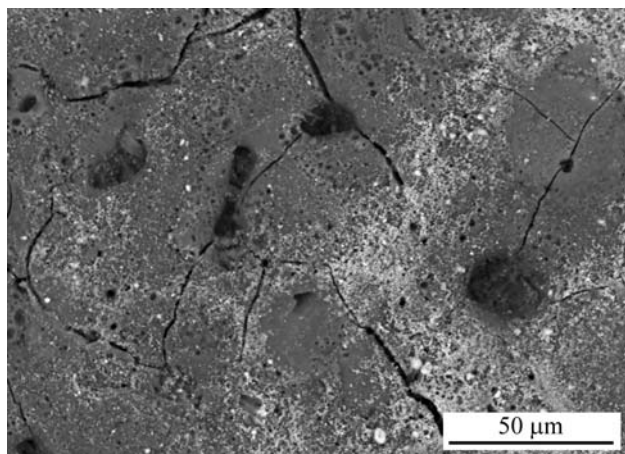
Fig. 5 Scanning electron micrograph (backscattered electrons) of a plan view of magnesium following PEO treatment for 2,400 s at 3 A dm^{-2} in 0.025 M Na$_3$PO$_4 \cdot$ 12H$_2$O/1.5 M NH$_4$OH electrolyte, with addition of 2 g L^{-1} of zirconia particles

heterogeneous particle distribution is uncertain. However, the size of depleted regions is in the range of microdischarge dimensions. Thus, the depleted regions may represent areas where particles are being re-accumulated following earlier microdischarges that incorporated surface zirconia particles into the coating or possibly displaced some zirconia from the surface.

Sequential PEO treatments were also carried out to confirm the sites of incorporation of zirconia particles in the coatings. A coating was produced of average thickness ∼15 μm by PEO treatment for 900 s in zirconia-free phosphate electrolyte, and then further thickened, to ∼20 μm, by treatment for 300 s in zirconia-containing phosphate electrolyte. Similarly to treatment in the

individual electrolytes, cross-sections disclosed particles concentrated at the coating surface and the inner coating material (Fig. 6). A mixed phase microstructure was resolved locally in the outer coating material, due to redistribution of zirconium in discrete regions. The modified microstructure extended throughout the thickness of the layer in certain places. The extent of microstructural transformation of the outer layer probably depends upon the local temperature rise and local amounts of zirconia.

Discussion

Incorporation of zirconia particles

The findings of the study reveal the incorporation of zirconia particles into PEO coatings on magnesium and their structural and compositional transformation, which is evident from the identification of tetragonal zirconia and Mg$_2$Zr$_5$O$_{12}$ and microstructural changes in the outer coating material. As indicated in the phase diagram for ZrO$_2$–MgO (Fig. 7), the monoclinic, tetragonal, and cubic forms of zirconia are stable to 1,513, 2,643, and 2,988 K respectively [20]. In comparison, the melting points of MgO and magnesium are 3,098 and 923 K, respectively. The boiling point of magnesium is 1,363 K. Magnesium oxide can stabilize the cubic form of zirconia, although none was detected in the present coatings. The incidence of tetragonal zirconia in the coatings suggest local temperature rise to at least 1,513 K. Further, the morphologies of particles at the surface and within the coating are similar to those of the original particles, possibly due to temperatures
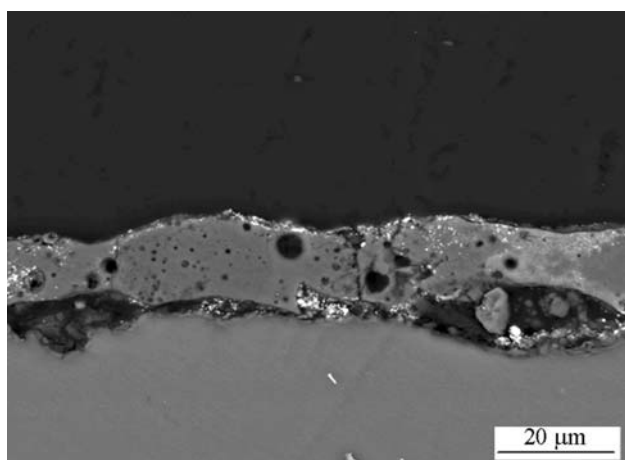

Fig. 6 Scanning electron micrograph (backscattered electrons) of a cross-section of magnesium following PEO treatment for 900 s at 3 A dm^{-2} in 0.025 M Na$_3$PO$_4 \cdot$ 12H$_2$O/1.5 M NH$_4$OH electrolyte, followed by further treatment for 300 s in the same electrolyte with addition of 2 g L^{-1} of zirconia particles

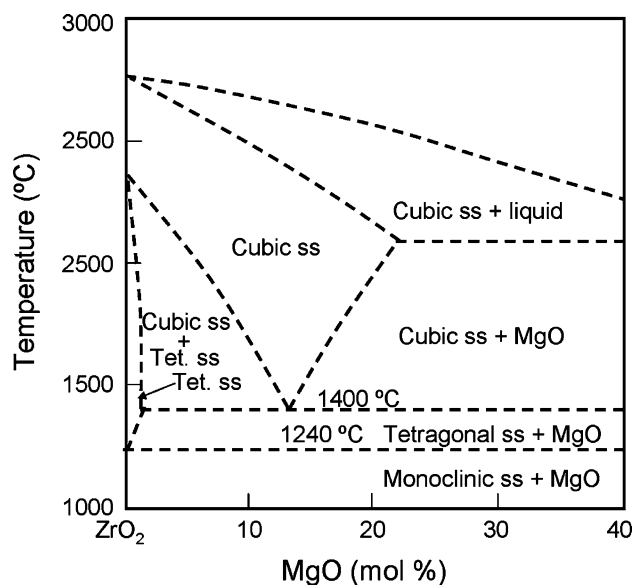**Fig. 7** ZrO$_2$–MgO phase diagram (ss = solid solution) [20]

remaining below the melting temperature of zirconia at the particular locations. The detection of monoclinic zirconia in the coatings may arise from untransformed original particles or due to a tetragonal-to-monoclinic transformation during cooling. A barrier-like layer next to the metal/coating interface appears to prevent particles reaching the metal. However, it is possible that this layer forms at the later stages of the breakdown process, when the microdischarge at a particular site is in its terminal stage and the local temperatures of the coating and the substrate are reducing back to the relatively low values of a microdischarge-free region. Zirconia particles are also present at the coating surface, although the amounts visible in cross-sections appear to be less than within the inner coating region.

Formation of the coatings

The mechanism of formation of the coating proceeds with initial growth of a barrier film in the period of approximately linear voltage rise of the voltage-time response. Barrier anodic films typically thicken at a formation ratio of ~ 1 nm V^{-1}, with the electric field driving transport of cations and anions across the barrier layer. A formation of ~ 0.6 nm V^{-1} has been reported for magnesium [21]. The present barrier films are therefore expected to achieve thicknesses of ~ 100–200 nm at the onset of sparking, at 170 and 225 V in silicate and phosphate, with further increase in thickness possible at later stages of treatment as final voltages rise toward ~ 500 V. The early stages of growth of the barrier films occur with relatively uniform flow of current through the film. However, particularly with initiation of microdischarges, current flow becomes concentrated at the breakdown sites, probably associated with flaws in the barrier layer. Local Joule heating probably leads to local thickening and cracking of the barrier layer [22]. Previous study of WE43 alloy revealed the formation of layered-type coatings, similar to those found in the present work, soon after the initiation of microdischarges [10]. Further, the main coating layers thickened progressively with time of treatment, the inner layer being typically ~ 30–40% of the total coating thickness. The inner layer material containing silicon species, following formation in silicate electrolyte, was substituted relatively quickly by phosphorus-containing material following further treatment in phosphate electrolyte. However, the composition of the outer material changed more slowly than that of the inner region. The behavior indicated readily transport of electrolyte constituents to the inner coating. However, the mechanism of formation of the inner coating layer is uncertain, and may involve a combination of anodic, plasma, and thermal oxidation processes. The outer layer, which is clearly heated to elevated temperatures resulting in relatively complex ceramic microstructures, contains magnesium species derived from the substrate, suggesting transport of species from the inner coating layer. The relative thickness of coating layers can be modified by treatment under AC or pulsed voltage conditions, which affects the duration of microdischarges [23].

The distributions of zirconia particles within the present coatings suggest that a main route of incorporation of zirconium species into the coating is through short-circuit paths in the outer layer, similar to previous findings for silicon and phosphorus species originating from anions of the electrolyte [8, 10]. The transport paths are probably breakdown channels, together with cracks and pores in the coatings. The outer and inner coating materials are heated sufficiently by the high local current density for transformation of the monoclinic zirconia to the tetragonal form and for formation of $Mg_2Zr_5O_{12}$ phase [24]. The latter phase, which has been reported to form at temperatures between 2,123 K and 2,373 K, was only found in the coating formed in phosphate electrolyte. The absence of detectable quantities of $Mg_2Zr_5O_{12}$ in the coating formed in silicate electrolyte probably reflects differing ratios of coating constituents and thermal conditions at sites of microdischarges in the two coatings, with the voltage being lower at a particular time during coating growth in the silicate electrolyte. The relative ease of transport of species along short-circuit paths suggests that the main voltage drop occurs in the inner layer regions. Accordingly, greatest heating may be generated in the inner coating, which may lead to melting. Heat will be dissipated through the outer coating to the electrolyte and to the metal substrate. The outer layer possibly forms by deposition of higher melting point constituents of the inner coating at the inner/outer coating interface. Further, under the locally high temperature, diffusion of coating species, transport of coating species along cracks and pores, and formation of new phases may take place in the outer layer. The coating material may also flow under the stresses generated by coating formation to fill pores and cracks.

The presence of zirconia particles at the surface of the coatings suggests that coating growth can also proceed at this interface. The zirconia particles may originate indirectly from transport of the inner coating material by flow along short-circuit paths or directly from the electrolyte, for instance by deposition following solution boiling or following transport to the surface by electrophoresis, due to the electric field in the electrolyte close to the coating surface. The outer coating material appears to partially envelop the particles, with small craters being evident where particles have been dislodged. Particles may also be entrained within silicon-rich material that forms at the surface of coatings produced in silicate electrolyte.

Conclusions

1. Zirconia particles are incorporated into coatings formed by DC PEO treatments of magnesium in phosphate and silicate electrolytes at the coating surface and within the inner coating layer.
2. Short-circuit transport paths are present within the outer coating layer that allow access of electrolyte constituents, including anionic and particulate components, to the inner coating regions.
3. Local temperature rise to at least 1,513 K results in transformation of zirconia from the monoclinic to tetragonal form and compositional and microstructural changes in the outer coating layer due to incorporation of zirconium species.

References

1. Nykyforchyn HM, Klapkiv MD, Posuvailo VM (1998) Surf Coat Technol 100–101:219
2. Matykina E, Monfort F, Berkani A, Skeldon P, Thompson GE, Chapon P (2006) Philos Mag 86:49
3. Kuhn A (2003) Met Finish 101:44
4. Blawert C, Dietzel W, Ghali E, Song G (2006) Adv Eng Mater 8:511
5. Monfort F, Berkani A, Matykina E, Skeldon P, Thompson GE, Habazaki H, Shimizu K (2007) Corros Sci 49:672
6. Nie X, Meletis EJ, Jiang JC, Leyland A, Yerokhin AL, Matthews A (2002) Surf Coat Technol 149:245
7. Belevantsev VI, Terleeva OP, Markov GA, Shulepko EK, Slonova AI, Utkin VV (1998) Prot Met 34:469
8. Monfort F, Berkani A, Matykina E, Skeldon P, Thompson GE, Habazaki H, Shimizu K (2005) J Electrochem Soc 152:C382
9. Matykina E, Doucet G, Monfort F, Berkani A, Skeldon P, Thompson GE (2006) Electrochim Acta 51:4709
10. Arrabal R, Matykina E, Skeldon P, Thompson GE, Pardo A (2007) J Electrochem Soc (in press)
11. Saifullin RS (1992) Physical chemistry of inorganic polymeric and composite materials. Ellis Horwood, New York, p 238
12. Bakovets VV, Polyakov OV, Dolgovesova IP (1991) Plasma electrolytic anode treatment of metals (in Russian), Nauka, Novosibirsk
13. Jin F, Chu PK, Tong H, Zhao J (2006) Appl Surf Sci 253:863
14. Butyagin P, Khokhryakov Y, Mamaev A (2003) Mater Lett 57:1748
15. Liang J, Hu L, Hao J (2007) Electrochim Acta 52:4836
16. Fukumasa O, Tagashira R, Tachino K, Mukunoki H (2003) Surf Coat Technol 169–170:579
17. Wachtman JB, Haber RA (1993) Ceramic films and coatings. William Andrew Publishing/Noyes, New Jersey, p 143
18. Hannink RH (1983) J Mater Sci 18:457
19. Xie L, Ma X, Jordan EH, Padture NP, Xiao DT, Gell M (2004) J Mater Sci 39:1639
20. Grain CF (1967) J Am Ceram Soc 50:288
21. Khaselev O, Yahalom J (1998) Corros Sci 40:1149
22. Shimizu K, Thompson GE, Wood GC (1982) Thin Solid Films 92:231
23. Yerokhin AL, Shatrov A, Samsonov V, Shashkov P, Pilkington A, Leyland A, Matthews A (2005) Surf Coat Technol 199:150
24. Liu Z, Spargo AE (2001) Philos Mag A 81:625